

## REVIEW

## Advances in neuroimaging in frontotemporal dementia

Elizabeth Gordon, Jonathan D. Rohrer and Nick C. Fox

*Dementia Research Centre, Department of Neurodegenerative Disease, UCL Institute of Neurology, London, UK*

## Abstract

Frontotemporal dementia (FTD) is a clinically and neuroanatomically heterogeneous neurodegenerative disorder with multiple underlying genetic and pathological causes. Whilst initial neuroimaging studies highlighted the presence of frontal and temporal lobe atrophy or hypometabolism as the unifying feature in patients with FTD, more detailed studies have revealed diverse patterns across individuals, with variable frontal or temporal predominance, differing degrees of asymmetry, and the involvement of other cortical areas including the insula and cingulate, as well as subcortical structures such as the basal ganglia and thalamus. Recent advances in novel imaging modalities including diffusion tensor imaging, resting-state functional magnetic resonance imaging and molecular positron emission tomography imaging allow the possibility of investigating alterations in structural

and functional connectivity and the visualisation of pathological protein deposition. This review will cover the major imaging modalities currently used in research and clinical practice, focusing on the key insights they have provided into FTD, including the onset and evolution of pathological changes and also importantly their utility as biomarkers for disease detection and staging, differential diagnosis and measurement of disease progression. Validating neuroimaging biomarkers that are able to accomplish these tasks will be crucial for the ultimate goal of powering upcoming clinical trials by correctly stratifying patient enrolment and providing sensitive markers for evaluating the effects and efficacy of disease-modifying therapies.

**Keywords:** frontotemporal dementia, neuroimaging.  
*J. Neurochem.* (2016) **138** (Suppl. 1), 193–210.

*This article is part of the [Frontotemporal Dementia special issue](#).*

Frontotemporal dementia (FTD) is a clinically, genetically and pathologically heterogeneous neurodegenerative disorder (Seelaar *et al.* 2011) and a common cause of early onset dementia (Onyike and Diehl-Schmid 2013). Clinically, patients present with either changes in behaviour and

personality (behavioural variant FTD, bvFTD), or language impairment (primary progressive aphasia, PPA). PPA can be further divided into three main subtypes, semantic variant (svPPA), non-fluent variant (nfvPPA), and logopenic variant (lvPPA) (Gorno-Tempini *et al.* 2011). As the disease

Received February 17, 2016; revised manuscript received May 2, 2016; accepted May 3, 2016.

Address correspondence and reprint requests to Dr Jonathan D. Rohrer, Dementia Research Centre, Department of Neurodegenerative Disease, UCL Institute of Neurology, Queen Square, London, WC1N 3BG, UK. E-mail: j.rohrer@ucl.ac.uk

**Abbreviations used:** AD, Alzheimer's disease; AD, axial diffusivity; ANT, anterior; ASL, arterial spin labelling; AUC, area under the curve; bvFTD, behavioural variant frontotemporal dementia; C9orf72, chromosome 9 open reading frame 72; CBD, corticobasal degeneration; CBF, cerebral blood flow; CBS, corticobasal syndrome; dACC, dorsal anterior cingulate cortex; DIAN, Dominantly Inherited Alzheimer Network; DLPFC, dorsolateral prefrontal cortex; DMN, default mode network; DTI, diffusion tensor imaging; FA, fractional anisotropy; FDG-PET, fluorodeoxyglucose positron emission tomography; FEF, frontal eye fields; fMRI, functional magnetic resonance imaging; FTD-ALS, frontotemporal dementia with amyotrophic lateral sclerosis; FTD,

frontotemporal dementia; FUS, fused in sarcoma; GENFI, Genetic Frontotemporal dementia Initiative; GRN, progranulin; IC, insular cortex; IFG, inferior frontal gyrus; INF, inferior; LAT, lateral; lvPPA, logopenic variant of primary progressive aphasia; MAPT, microtubule-associated protein tau; MD, mean diffusivity; MED, medial; MRI, magnetic resonance imaging; nfvPPA, non-fluent variant of primary progressive aphasia; PCC, posterior cingulate cortex; PET, positron emission tomography; PIB, Pittsburgh compound B; POST, posterior; PPA, primary progressive aphasia; PPAOS, primary progressive apraxia of speech; PrC, precuneus; PSP, progressive supranuclear palsy; RD, radial diffusivity; SPECT, single-photon emission computed tomography; sPL, superior parietal lobule; SUP, superior; SUVR, standardised uptake value ratio; svPPA, semantic variant of primary progressive aphasia; TDP-43, TAR DNA-binding protein 43; VCP, valosin-containing protein; VMPFC, ventromedial prefrontal cortex; VOI, volumes of interest.

progresses, patients may also develop features of amyotrophic lateral sclerosis (FTD-ALS), corticobasal syndrome or progressive supranuclear palsy (PSP). FTD is highly heritable, with approximately a third of patients exhibiting an autosomal dominant form: mutations in the microtubule-associated protein tau (*MAPT*) and progranulin (*GRN*) genes and hexanucleotide expansions in the chromosome 9 open reading frame 72 (*C9orf72*) gene constitute the major causes (Rohrer *et al.* 2009a). Pathologically, neuronal inclusions usually contain abnormal forms of one of three proteins: tau, TAR DNA-binding protein 43 (*TDP-43*) or fused in sarcoma (*FUS*) (Mackenzie *et al.* 2010).

Early neuroimaging studies quantifying atrophy from volumetric magnetic resonance imaging (MRI) and hypometabolism, using 18F-fluorodeoxyglucose positron emission tomography (FDG-PET) revealed characteristic patterns of abnormalities across FTD subtypes, whilst recent advances in novel imaging modalities such as diffusion tensor imaging (DTI), resting-state functional MRI, arterial spin labelling (ASL) and tau PET imaging provide promising new techniques for investigating connectivity and molecular changes in these clinical, genetic and pathological subgroups. This review will cover the major imaging modalities currently used in research and clinical practice, focusing on the key insights they have provided into FTD, including the onset and evolution of pathological changes and also importantly their utility as biomarkers for disease detection and staging, differential diagnosis and measurement of disease progression. Validating neuroimaging biomarkers that are able to accomplish these tasks will be crucial for the ultimate goal of powering upcoming clinical trials by correctly stratifying patient enrolment and providing sensitive markers for evaluating the effects and efficacy of disease-modifying therapies.

## Neuroanatomical signatures of FTD

### Differing distributions: visualising structural loss using volumetric 3D T1 MRI

There is a considerable body of research employing volumetric MRI to investigate the pattern and distribution of cerebral loss (often with a focus on grey matter) in FTD. The majority of studies have been aimed at improving differential diagnosis, both distinguishing FTD from other neurodegenerative conditions such as Alzheimer's disease (AD), as well as differentiating between the clinical, pathological and genetic subtypes within the FTD spectrum.

### Clinical syndromes

Volume loss in bvFTD occurs primarily in the frontal and temporal lobes. Several meta-analyses have highlighted the particular involvement of the prefrontal cortex, anterior temporal regions, the insula, anterior cingulate, striatum and thalamus (Fig. 1) (Schroeter *et al.* 2007; Pan *et al.* 2012), a

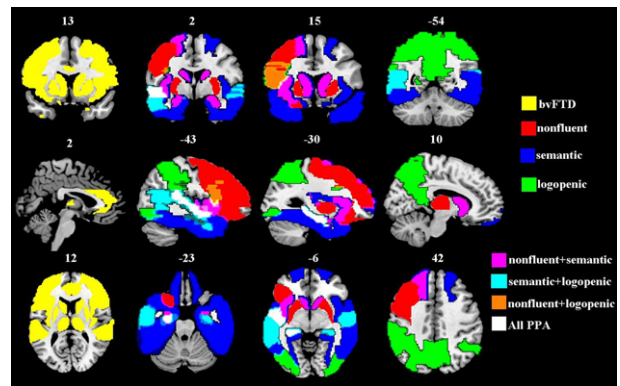


**Fig. 1** Characteristic patterns of grey matter atrophy in the four major clinical FTD subtypes, overlaid on a rendered 3D surface of the Montreal Neurological Institute Template brain. Representative coronal, sagittal and axial slices are displayed in the first, second and third rows respectively. Images reproduced from Agosta *et al.* 2012a.

pattern that has high sensitivity and specificity in differentiating bvFTD from AD (Schroeter *et al.* 2007). Despite a general consensus in the regional pattern of involvement at the group level, one important issue is the significant heterogeneity of individual findings, with cases having a variable degree of hemispheric asymmetry, differing predominance of frontal versus temporal lobe atrophy and a varying extent of posterior cortical involvement (Schroeter *et al.* 2014). To address this, two cluster analyses have been performed, which suggest that at least four neuroanatomical subtypes of bvFTD exist: two with predominantly frontal atrophy (a focal frontal-dominant and a more distributed frontotemporal subtype) and two with predominantly temporal involvement (including a focal temporal-dominant and a more widespread temporo-frontal-parietal subtype), which potentially map onto distinct pathogenetic causes of FTD (Whitwell *et al.* 2009b, 2012).

In contrast, svPPA patients have a much more characteristic pattern of asymmetric temporal lobe atrophy, primarily in the anterior and inferior regions (Gorno-Tempini *et al.* 2004; Rohrer *et al.* 2009b). The most common presentation is prominent left-sided atrophy, although a right-dominant variant has been described (Chan *et al.* 2009; Josephs *et al.* 2009). Earliest changes include grey matter loss in the inferior temporal and fusiform gyri, the temporal pole and the parahippocampal and entorhinal cortex (Fig. 1) (Brambati *et al.* 2009; Rohrer *et al.* 2009b; Rogalski *et al.* 2011). These changes can be striking at presentation with the MRI revealing advanced temporal pole atrophy despite the patient's general maintenance of activities of daily living. Involvement of the amygdala and hippocampus has also been reported (Schroeter *et al.* 2007). With increasing severity, this pattern extends anteriorly to include orbitofrontal, inferior frontal, insular and anterior cingulate cortices, as well as posteriorly to include temporoparietal regions, and

corresponding regions in the contralateral hemisphere (Rohrer *et al.* 2009b).

Atrophy profiles in nfvPPA also include predominantly left hemisphere cortical regions of loss; however, the distribution distinguishes it from svPPA (Gorno-Tempini *et al.* 2004; Rogalski *et al.* 2011). These include changes in the inferior frontal gyrus (particularly the pars opercularis), dorsolateral prefrontal cortex, superior temporal gyrus and insula (Fig. 1). Over time, this pattern of cortical loss includes prefrontal and temporal lobe structures in the right hemisphere as well as continued propagation ipsilaterally to encompass anterior frontal, lateral temporal and anterior parietal lobes (Rohrer *et al.* 2009b; Rogalski *et al.* 2011), with involvement of caudate and putamen bilaterally (Gorno-Tempini *et al.* 2004).

In contrast to both svPPA and nfvPPA, the logopenic variant of PPA presents with a significantly more posterior profile, involving early left temporoparietal and posterior cingulate atrophy (Gorno-Tempini *et al.* 2004; Rogalski *et al.* 2011) (Fig. 1).

In summary, investigations based on clinical syndromes have proven useful in elucidating broadly distinct and dissociable patterns of atrophy that correspond well with the behavioural and language disturbances that are associated with the syndromes. However, considerable individual variability within these groups and some overlap of regional involvement occurs, likely reflecting the significant heterogeneity of genetic contributions and pathological processes underpinning the disease. When this information is available, investigations including these levels of classification have proved highly valuable in extending our understanding of FTD.

### Genetic forms

Patients with *MAPT* mutations present primarily with focal symmetrical anterior temporal and orbitofrontal lobe atrophy (Fig. 2). Caudate, insula and anterior cingulate involvement

has also been reported (Spina *et al.* 2008; Ghetti *et al.* 2015). In addition, preliminary findings suggest a more lateral temporal lobe signature for *MAPT* mutations in the coding region, while those affecting the splicing of exon 10 target the medial temporal lobes (Whitwell *et al.* 2009a). In these latter cases, the marked symmetrical loss of hippocampal volume may cause confusion with AD (Tolboom *et al.* 2010; Liang *et al.* 2014). Unlike *MAPT*, *GRN* mutations commonly present with markedly asymmetric atrophy of the temporal, inferior frontal and inferior parietal lobes (Rohrer *et al.* 2010b; Whitwell *et al.* 2012). Finally, *C9orf72* mutations show a more distributed symmetric pattern of atrophy, predominantly involving dorsolateral and medial frontal and orbitofrontal lobes, with additional loss in anterior temporal, parietal and occipital lobes, as well as in the thalamus and cerebellum (Mahoney *et al.* 2012a,b; Sha *et al.* 2012). These atrophy profiles not only differentiate *MAPT*, *GRN* and *C9orf72* patients at the group level, but have shown some success in classifying the different mutation carriers at the single-subject level (Whitwell *et al.* 2012).

### Pathologically defined forms

Given that future therapeutic interventions will likely target the abnormal proteins underpinning the disease, a key challenge is finding neuroanatomical signatures that can accurately predict molecular pathology non-invasively during life. Recent advances in classifying the subtypes of these FTD pathologies have contributed greatly to this goal (Fig. 2). In the tauopathies, *Pick's disease* can be associated with often striking asymmetric atrophy in the frontal cortex (including orbitofrontal, medial, and dorsolateral regions primarily), with involvement of the anterior temporal lobes and insula as well (Rankin *et al.* 2011; Whitwell *et al.* 2011a). *PSP* is associated classically with midbrain atrophy (Massey *et al.* 2013); however, despite being relatively specific, this is not a sensitive marker. Moreover, in patients with cognitive presentations, *PSP* and corticobasal

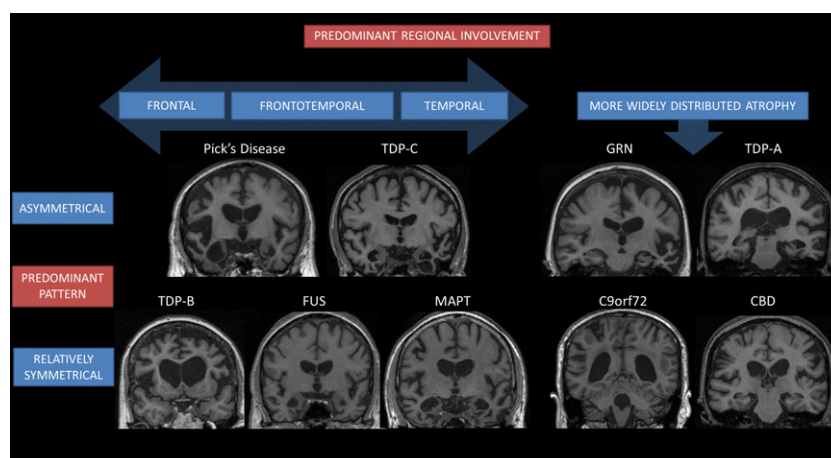


**Fig. 2** Coronal T1 volumetric MR images displaying characteristic patterns and distribution of regional volume loss for each of the main genetic and pathological subtypes of FTD.

degeneration tauopathies are associated with more posterior frontal cortical atrophy, targeting the supplementary and pre-motor regions, with corticobasal degeneration showing a more distributed pattern, including the parietal lobes and striatum (Josephs *et al.* 2008; Whitwell *et al.* 2010a).

*TDP-43* proteinopathies can be divided into four distinct subtypes (*Types A–D*), based on morphology of the inclusions (Mackenzie *et al.* 2011). Patients with *TDP-A* pathology (commonly associated with *GRN* mutations) present with widespread asymmetric frontotemporoparietal atrophy (Rohrer *et al.* 2010a; Whitwell *et al.* 2010b), with anterior cingulate and caudate involvement (Rohrer *et al.* 2011). *TDP-B* patients present with symmetrical frontal lobe as well as insula and anteromedial temporal lobe atrophy, whilst in contrast, *TDP-C* patients show asymmetrical loss in the anteroinferior temporal lobe, consistent with the predominant clinical diagnosis of svPPA (Rohrer and Rosen 2013). *TDP-D* is by far the rarest variant and associated with mutations in the valosin-containing protein gene. Preliminary MRI findings have been inconsistent and failed to demonstrate a clear pattern (Stojkovic *et al.* 2009; Kim *et al.* 2011; Surampalli *et al.* 2015).

Although rare, investigations into fused in sarcoma pathology cases reveal a pattern of atrophy affecting the orbitofrontal lobe, anteromedial temporal lobe, anterior cingulate, insula and particularly striking caudate atrophy (Fig. 2) (Josephs *et al.* 2010; Seelaar *et al.* 2010; Rohrer *et al.* 2011).

In summary, structural imaging provides a valuable tool for capturing neuroanatomical signatures in the clinical, genetic and pathological subgroups of FTD. The profiles commonly correspond well with the clinical presentation and, despite overlap, provide useful tools for differentiating subtypes at the group, and in some cases individual, subject level. However, inconsistencies in the literature exist and volumetric MRI changes may well be visible only after significant neuronal loss. In contrast, measures of regional brain activity may provide greater sensitivity to degenerative disease by detecting deterioration of neuronal function prior to cell loss (Jack *et al.* 2010).

### A loss of connection Part 1: viewing functional networks with resting-state fMRI

There is increasing focus on network-led frameworks for understanding the distribution and impact of neurodegeneration. Resting-state fMRI can be used to elucidate functionally connected brain networks by measuring synchronised time-dependent fluctuations in blood oxygenation levels (BOLD signal) as a surrogate measure of coordinated neural activity. Different patterns of correlated activation can detect spatially distinct, but functionally related, networks of cortical and subcortical regions (Seeley *et al.* 2009). The key functional networks implicated in

FTD are the default mode network, the language and semantic networks distributed predominantly across the left hemisphere, and the salience and executive control networks (Fig. 3) (Pievani *et al.* 2011; Lee *et al.* 2014). In bvFTD, multiple studies have described reduced connectivity in the salience network, which includes the frontal lobe, anterior cingulate, insula, amygdala, medial thalamus and ventral striatum, all regions involved in evaluating emotional significance and appropriately contextualising responses (Seeley *et al.* 2007; Farb *et al.* 2013). It has been proposed that reduced connectivity in the salience network may result in compensatory increased connectivity within the default mode network (Zhou *et al.* 2010; Whitwell *et al.* 2011b; Borroni *et al.* 2012; Farb *et al.* 2013). However, this finding has not been consistent across all studies of bvFTD patients (Filippi *et al.* 2013). In svPPA, reduced functional connectivity particularly affecting a semantic network involving the left anterior temporal lobe has been shown (Guo *et al.* 2013), along with inferior and ventral regions of the temporal lobe, bilateral frontal cortex, left amygdala, hippocampus, caudate and occipital regions (Agosta *et al.* 2014). Despite few investigations of nvPPA, there is preliminary evidence for reduced functional connectivity in the frontal operculum, primary and supplementary motor areas and inferior parietal lobule, linking the language and motor networks that enable fluent speech (Seeley *et al.* 2009).

In summary, studies on functional connectivity in FTD demonstrate that anatomical regions affected by specific phenotypes show abnormalities in related functional connectivity networks. Whilst the use of resting-state fMRI has proven robust in differentiating bvFTD from AD patients (Zhou *et al.* 2010; Zhou and Seeley 2014), more work is required in comparing clinical subtypes and in genetic and pathologically confirmed cohorts to improve the utility of this promising technique in FTD.

### A loss of connection Part 2: structural connectivity investigations with DTI

Investigating alterations in key white matter structural connections (Fig. 4) is of particular interest in understanding propagation of neurodegeneration (Warren *et al.* 2013). DTI allows the visualisation of these structural networks by measuring directionality (fractional anisotropy) and level of diffusivity (mean, radial and axial) of water in the brain. Water diffuses differently depending on tissue type, neural integrity and presence of barriers such as myelinated fibres, enabling modelling of the architecture of neuronal connections (Soares *et al.* 2013). High fractional anisotropy (FA) indicates intact connected fibres, as water diffusion is restricted directionally along these tracts. A decrease in FA and increase in diffusivity therefore suggests degeneration of these directional fibres and loss of structural connectivity within the brain.

**Fig. 3** Representative regional distribution of the salience, default mode and executive control functional networks. Abbreviations: dACC, dorsal anterior cingulate cortex; VMPFC, ventromedial prefrontal cortex; PCC, posterior cingulate cortex; PrC, precuneus; DLPFC, dorsolateral prefrontal cortex; IC, insular cortex; sPL, superior parietal lobule; Image adapted from Hoefft *et al.* 2012.

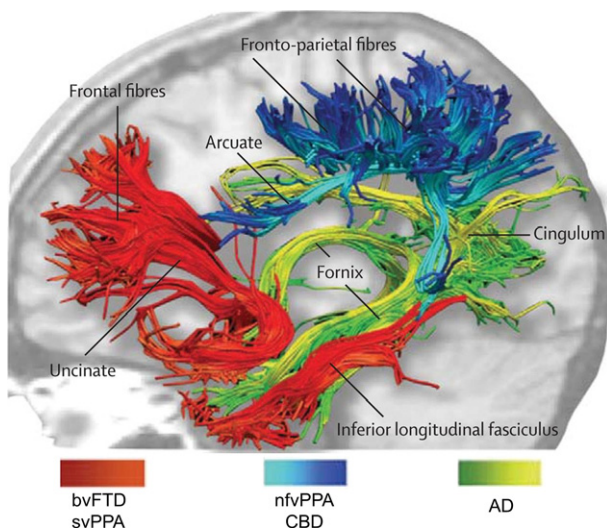
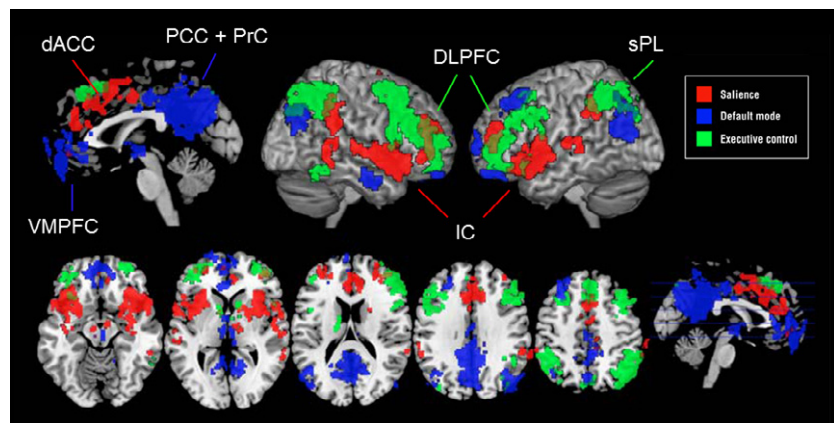


**Fig. 4** Main white matter tracts affected in bvFTD, svPPA, nfvPPA, CBD and Alzheimer's disease. Images adapted from Catani and Mesulam 2008.

In bvFTD, patients present with widespread reduction in FA and increased diffusivity metrics in tracts with reciprocal connections to the frontal and temporal lobes. Key tracts include the uncinate fasciculus, the genu of the corpus callosum (with an anterior-posterior gradient) and cingulum (Agosta *et al.* 2012b; Mahoney *et al.* 2015). Alterations in the anterior parts of the superior and inferior longitudinal fasciculi and inferior fronto-occipital fasciculus have also been reported (Diehl-Schmid *et al.* 2014), connecting grey matter regions shown to be predominantly atrophied in bvFTD and implicated in the key behavioural symptoms (Cerami and Cappa 2013).

For bvFTD patients with a *MAPT* mutation, the cingulum and uncinate fasciculus are particularly affected (Mahoney *et al.* 2014). Uncinate fasciculus abnormalities have also been demonstrated in presymptomatic *MAPT* mutation carriers (Dopper *et al.* 2013) suggesting a particular early vulnerability in these tracts. In *C9orf72* mutation carriers, FA

reductions have been shown in the superior cerebellar peduncles, consistent with previous findings of cerebellar atrophy in *C9orf72* patients (Mahoney *et al.* 2012a,b), a region previously thought to be relatively preserved in FTD.

The PPA groups show more focal and asymmetric white matter changes in specific networks fundamental to language processing. In svPPA, left frontotemporal abnormalities dominate, including the left uncinate fasciculus and inferior longitudinal fasciculus tracts (Mahoney *et al.* 2013; Tu *et al.* 2016). Additional regions include corpus callosum and cingulum, with sparing of the occipital white matter, brainstem, and cerebellum (Galantucci *et al.* 2011; Agosta *et al.* 2012a,b; Lam *et al.* 2014). Decreased FA and increased diffusivity is somewhat more distributed in nfvPPA with predominantly left frontotemporoparietal abnormalities. Tracts and subcomponents affected include the left superior longitudinal fasciculus, the corpus callosum, left cingulum, left orbitofrontal, inferior frontal, anterior temporal, and inferior parietal white matter regions (Galantucci *et al.* 2011; Agosta *et al.* 2012a,b). In keeping with the distribution of grey matter volume loss, white matter abnormalities in lvPPA variants demonstrate left frontoparietal predominance, including the left superior longitudinal fasciculus/arcuate fasciculus particularly (Agosta *et al.* 2012b).

DTI measures show promise in sensitivity analyses for differentiating FTD from control subjects, as well as between the subgroups. However, there is some inconsistency in precisely which combination of DTI metrics and tracts produces the best predictors and will need further investigation to improve utility as a marker for differential diagnosis (Agosta *et al.* 2012a,b; Mahoney *et al.* 2015). DTI metrics also show promise as markers identifying earliest pathogenic changes in FTD. The key white matter tracts demonstrating abnormalities are connected to regions of significant grey matter loss in the syndromic variants, but often more extensively, suggesting that alterations in white matter integrity precede structural changes. This is further supported by presymptomatic studies detecting white matter changes in

the absence of grey matter abnormalities (Borroni *et al.* 2008; Dopfer *et al.* 2013). Further investigation including pathologically confirmed and larger cohorts of genetic presymptomatic patients will strengthen the current findings and determine the best method for measuring the earliest change. In addition, valid methods for pooling findings into meta-analyses of DTI data are currently lacking and will be highly valuable for further clarification of findings.

#### Altered uptake: imaging loss of metabolism

PET with [<sup>18</sup>F] fluorodeoxyglucose (FDG-PET) and perfusion single-photon emission computed tomography (SPECT) are widely utilised methods for investigating patterns of cerebral glucose metabolism or cerebral perfusion as measures of neuronal (dys)function. FDG-PET has been found to have greater utility than SPECT (Davison and O'Brien 2014). The patterns of hypometabolism tend to accord closely with patterns of atrophy (Fig. 5). Numerous FDG-PET studies, including those with post-mortem pathological confirmation demonstrate high sensitivity and specificity in aiding differential diagnosis of AD and FTD (Foster *et al.* 2007; Panegyres *et al.* 2009; Rabinovici *et al.* 2011; Davison and O'Brien 2014) as well as promise in differentiating FTD subtypes (Matias-Guiu *et al.* 2014). Hypometabolism in the frontotemporal regions is commonly found in bvFTD patients, particularly affecting the orbitofrontal, dorsolateral and medial prefrontal cortex and anterior temporal poles (Diehl-Schmid *et al.* 2007; Ishii 2014; Verfaillie *et al.* 2015). Involvement of the hippocampus, anterior cingulate, basal ganglia, anterior insula and thalamus have been less consistently reported, most likely because of variability in techniques, underlying pathology and disease severity between studies (Schroeter *et al.* 2007; Mosconi *et al.* 2008). In svPPA patients, temporal lobe hypometabolism predominates, with asymmetrical left hemisphere involvement in the entorhinal and perirhinal cortex, inferior temporal

poles and amygdala (Desgranges *et al.* 2007; Diehl-Schmid *et al.* 2006). For nfvPPA patients, more pronounced hypometabolism is evident, particularly in the left inferior frontal and superior temporal regions (Rabinovici *et al.* 2008). Finally, lvPPA subjects show distributed left frontotemporoparietal hypometabolism, particularly involving lateral frontal and posterior-lateral temporal lobes, alongside caudate, posterior cingulate and precuneus regions (Rabinovici *et al.* 2008; Madhavan *et al.* 2013; Josephs *et al.* 2014).

In summary, FDG-PET and SPECT have been widely used to assess regional metabolic changes in FTD and have value in differential diagnosis and early detection of pathogenic abnormalities. However, the degree of overlap of hypometabolism across the FTD spectrum and how distinct patterns map onto particular genetic and pathological subtypes is not well understood and will require further investigation. Despite its advantages, FDG-PET involves exposure to ionising radiation, is expensive and is not widely available, which limits its clinical utility. There are also methodological issues regarding correction for atrophy/partial volume effects during analysis. An alternative for measuring regional cerebral dysfunction is ASL MRI to assess cerebral blood flow deficits.

#### Patterns of perfusion: ASL demonstrates altered cerebral blood flow

Although currently underutilised, ASL imaging can be employed to assess cerebral blood flow using magnetically labelled arterial blood H<sub>2</sub>O as an endogenous marker. Advantages include relatively short acquisition time, no exposure to radiation, non-invasiveness, relatively low cost and wide availability. As with FDG-PET, the majority of investigations have been focused on investigating its utility in differential diagnosis of FTD from AD (Binnewijzend *et al.* 2014). Patients with bvFTD show bilateral frontal and

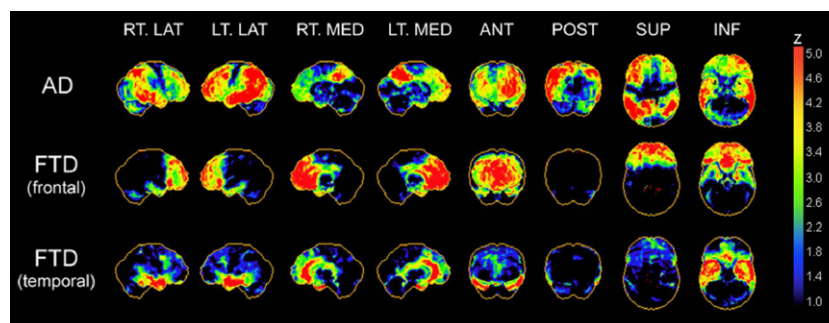


**Fig. 5** Distribution of typical hypometabolism profiles acquired using FDG-PET in Alzheimer's disease (AD) patients and patients with frontal and temporal FTD. Patterns are presented as z-score maps demonstrating voxels of significant hypometabolism compared with healthy controls. The focal frontal and temporal pattern of

hypometabolism in the FTD subgroups can be clearly distinguished from the distributed and posterior profile of temporoparietal hypometabolism evident in AD. ANT, anterior; INF, inferior; LAT, lateral; MED, medial; POST, posterior; SUP, superior. Reproduced from Bohnen *et al.*, 2012.

anterior cingulate hypoperfusion, whereas AD patients present with a more posterior profile including the medial parietal regions, posterior cingulate and the precuneus (Hu *et al.* 2010; Shimizu *et al.* 2010). The presence of posterior cingulate hypoperfusion has recently been shown to be a sensitive early stage differential diagnostic marker in separating AD from bvFTD (Steketee *et al.* 2015). In general, the patterns detected correlate well with changes in metabolism (Verfaillie *et al.* 2015) and thus ASL shows promise as a future alternative to FDG-PET, particularly in multimodal imaging approaches, although similar methodological issues to FDG-PET exist in analysing ASL data. To date, only a few studies utilising ASL in FTD and combined ASL/FDG-PET investigations exist, therefore further investigations are required to confirm the utility of ASL as a biomarker for differential diagnosis at the subgroup and individual subject level in FTD.

The imaging modalities discussed thus far provide insights into phenotypic and genotypic grey and white matter neuroanatomical signatures of disease. However, with few cases coming to post-mortem examination, much is still unknown about how these presentations map onto the underlying pathology driving the disease process. Deducing histopathology in patients often relies on a probabilistic combination of clinical features, neuroanatomical profile and what is currently known about the distribution of pathological burden. This model may prove useful at the group level, but prediction of single subject pathology is more difficult. Whilst definitive diagnosis can only be made from histopathological examination of brain tissue, molecular imaging provides a promising alternative to identifying pathology *in vivo*.

#### Molecular imaging of the moment: the place of amyloid PET

The development of PET-based imaging tracers, which bind to and thus demonstrate distribution of abnormal aggregations of amyloid in the brain, has proved valuable in visualising neuropathology *in vivo*. Several studies have shown the diagnostic utility of amyloid imaging in assisting differentiation of AD from FTD with relatively high sensitivity and specificity given that A $\beta$  plaques are a hallmark of AD and not within the FTD pathologic spectrum (Drzezga *et al.* 2008; Engler *et al.* 2008; Rabinovici *et al.* 2011; Villemagne *et al.* 2011). Most FTD patients reveal negative imaging findings for A $\beta$ , with the notable exception of lvPPA patients who usually have underlying AD pathology and therefore have amyloid tracer retention (Fig. 6) (Leyton *et al.* 2011; Mesulam *et al.* 2014). Several studies have also reported a small percentage of bvFTD, svPPA and nfvPPA patients with positive amyloid PET scans (Engler *et al.* 2008; Rabinovici *et al.* 2008; Villemagne *et al.* 2011). Classification was based on clinical diagnosis and thus without histopathological confirmation the positive imaging findings in FTD may reflect either misclassification or comorbid FTD and AD pathology.

Recently, one such mixed pathology case was reported where a positive florbetapir PET scan was exhibited while the patient was alive and diffuse amyloid neuritic plaques throughout the cerebral cortex, thalamus and striatum accompanied by frontal and temporal cortex *TDP-43* inclusions were observed post-mortem (Serrano *et al.* 2014). Coexisting FTD and AD pathology is more likely as people become older and so a positive amyloid scan is less helpful as age increases, particularly as amyloid positivity may be seen a number of years prior to symptoms of AD, and could therefore reflect prodromal AD rather than misdiagnosis.

In summary, amyloid imaging demonstrates confirmed utility in differentiating AD from FTD, even in the presence of overlapping clinical symptoms. Furthermore, it may prove useful in detecting atypical FTD presentations with underlying AD or mixed pathology. Its value is greatest in younger individuals because of the high prevalence of amyloid plaques in older populations. However, amyloid imaging does not help differentiate tau from *TDP-43* positive pathologies. Therefore, tracers targeting these FTD-specific pathologies *in vivo* will be invaluable for FTD research and stratification into future clinical trials.

#### Molecular imaging of the future: the place of tau PET

The recent development of PET ligands selective for tau pathology has clear potential for improving differential diagnosis in FTD as well as staging tau burden within the tauopathies. Furthermore, these tracers may provide important surrogate outcome measures for the efficacy of tau-targeted therapeutic interventions. There are several challenges for tau imaging: first, tau aggregates are mostly intracellular and so the tracer must successfully cross the blood–brain barrier and cell membrane to reach its target (Villemagne *et al.* 2015). Furthermore, the six different isoforms of tau present in altered combinations in different clinical phenotypes and tau aggregates are subject to a variety of post-translational modifications leading to diverse ultrastructural conformations (Sergeant *et al.* 2008). The candidate tracers must therefore be non-toxic, lipophilic molecules with low enough molecular weight to cross the cell membrane and must reversibly bind with high affinity to a variety of tau targets in a selective and specific manner (Villemagne and Okamura 2014). It is also preferable that these novel tau tracers be labelled with radioisotopes that exhibit a longer half-life, such as fluorine-18 ( $\approx 2$  h) to facilitate centralised production and distribution (Villemagne and Okamura 2016).

Few studies have been performed in FTD as of yet. A novel benzimidazole–pyrimidine derivative,  $^{18}\text{F}$ -T807 (now known as  $^{18}\text{F}$ -AV-1451) has been described (Xia *et al.* 2013; Chien *et al.* 2014), which exhibits greater than 25-fold selectivity for tau over A $\beta$  and preliminary findings from human trials have reported cortical retention matching known distribution of tau pathology in AD subjects (Chien

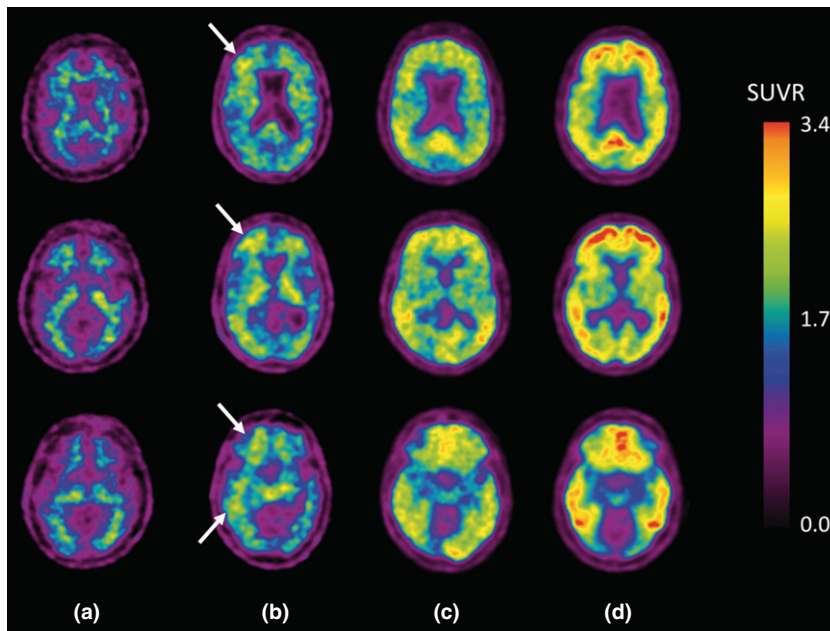


**Fig. 6** Representative examples of Pittsburgh Compound B (PiB) PET images. (a) PiB-PET negative retention indicating the lack of amyloid deposition. This is characteristic of bvFTD, svPPA and nfvPPA subjects. (b and c) demonstrate images from logopenic variant of primary progressive aphasia cases who had a positive scan (arrows indicate the cortical regions in (b) with a PiB-standardised uptake values ratio higher than 1.50) and (d) a positive scan from a typical AD case. SUVR, standardised uptake value ratio. Image reproduced from Leyton *et al.* 2011.

*et al.* 2013, 2014). Low retention in white matter results in high contrast images, ideal for visualising distribution of tau pathology (Villemagne *et al.* 2014). Studies have begun to analyse tauopathies including *MAPT* mutation carriers with  $^{18}\text{F}$ -AV-1451 PET. Preliminary results from a 56-year-old man with the P301L mutation demonstrates robust retention in characteristic frontotemporal regions (Ghetti *et al.* 2015) matching known tau pathology in these mutation carriers (Spina *et al.* 2008). This was detected three and a half years prior to the development of behavioural symptoms, suggesting sensitivity for early detection of abnormalities. However, it is important to note that there are reports of  $^{18}\text{F}$ -AV-1451 also binding to regions not known for tau deposition in AD patients as well as some discrepancies with *in vitro* studies reporting exclusive binding to paired helical filament-tau, whilst *in vivo* PET imaging demonstrating retention matching non-paired helical filament-tau aggregate distribution (Villemagne and Okamura 2016). These discrepancies highlight the need for future post-mortem validation of tau tracers to move this promising field of investigation forward.

In summary, tau PET imaging represents a significant advance in the imaging of neurodegeneration. It has great clinical potential for improved differential diagnosis and elucidating the evolution of tau deposition in the brain. Its potential to improve stratification into future trials will be crucial to power detection of a positive result (given initial effect sizes are likely to be small), and will also prove useful as a surrogate marker for evaluating tau-based therapies. Studies with autopsy confirmation as well as longitudinal investigations will be the next important steps for further validating this new imaging modality.

### Multiplying potential: multimodal imaging and advances in methodology

The combination of multiple neuroimaging techniques has recently shown promise for providing a more comprehensive picture of neurodegeneration. Initial investigations have demonstrated improved differentiation of AD from bvFTD patients (Avants *et al.* 2010), using combined measures of MRI grey matter cortical thickness with DTI metrics of white matter abnormalities. Combined MRI/DTI analyses have also demonstrated increased sensitivity and specificity for discriminating FTD and AD pathology (McMillan *et al.* 2012) as well as *tau* from *TDP-43* patients with autopsy confirmation or known genetic mutations (McMillan *et al.* 2013b). Furthermore, a study combining MRI, DTI and ASL found important differences in the impact of grey and white matter structural and functional abnormalities between AD and bvFTD patients, demonstrating potential value to improve differential diagnosis (Zhang *et al.* 2011). Recently, the application of combined MRI, DTI and resting-state fMRI in presymptomatic FTD mutation carriers showed different distributions of structural and functional connectivity changes in the frontotemporal grey and white matter structures in the absence of volumetric changes, providing valuable information about regions of earliest changes (Dopper *et al.* 2013).

Alongside these developments, it is worth noting that the emergence of increasingly sophisticated methods for modelling and analysing these combined neuroimaging datasets. Using combined MRI grey matter thickness and DTI, a recent study investigated the optimal neuroimaging classifiers to differentiate FTD and AD pathology (McMillan *et al.* 2014). Neuroimaging classifiers are based on three

categories: global measures (e.g. ventricular volume), regional anatomical volumes of interest (VOIs) (e.g. hippocampus) and a new technique for data-driven VOIs called eigenanatomy. Broadly speaking, this identifies and rank-orders clusters of voxels so that only regions that explain the greatest degree of variance in the imaging dataset are included. This has been shown to result in robust sets of predictors in classification studies, that are independent and not reliant on predetermined anatomical boundaries (McMillan *et al.* 2013a,b). Evaluations of classification accuracy using receiver operator characteristic analyses yielded the best results when combining data-driven VOIs and multi-modal imaging data achieving 89% sensitivity and 89% specificity (area under the curve = 0.874) for pathology classification of AD or FTD based on CSF total tau/A $\beta$ 42 findings. The same combination outperformed all others in the quantification of statistical power with the smallest estimated sample size of 26 required to perform accurate classification. This provides very promising results as a candidate biomarker for screening patients for entry into clinical trials.

#### A view across time: longitudinal investigations of rates of change

Whilst quantitative neuroimaging techniques have provided a wealth of information about neuroanatomical signatures in FTD, this work has been primarily cross-sectional. Despite the clear benefits of longitudinal study design, relatively few studies have investigated how these neuroanatomical profiles differentially change over time and even fewer have reported rates of disease progression within the FTD spectrum. Investigations characterising longitudinal trajectories of change in FTD are increasingly important as we move towards therapeutic trials in this patient population, not only to better characterise the evolution of the disease, but to provide surrogate markers for evaluating the efficacy of treatment interventions on slowing these degenerative trajectories.

Methods for quantifying brain atrophy rates from serial MRI are already currently employed as primary outcome measures in multiple clinical trials in AD (Cash *et al.* 2014) and are likely to feature in future trials enrolling FTD patients. Therefore, validation within this population is critical. Several studies have investigated rates of whole-brain loss and ventricular expansion across the clinical syndromes (Chan *et al.* 2001; Rohrer *et al.* 2008a, 2012; Knopman *et al.* 2009; Gordon *et al.* 2010). All have demonstrated significantly increased annual rates of change compared with healthy age-matched controls, employing the boundary shift integral (Freeborough and Fox 1997). Reported rates of annualised whole-brain loss have varied across studies and will need further validation in large well-characterised cohorts. However, there is broad agreement across studies that the PPA patients demonstrate more

homogeneous rates of global change compared with bvFTD (Chan *et al.* 2001; Rohrer *et al.* 2008a; Gordon *et al.* 2010), generally in the range of 2–3% of baseline brain volume (Table 1). Despite this global consistency in PPA, differences in hemispheric and lobar changes exist. One study suggests that left hemisphere rates are greater than right hemisphere rates for both svPPA and nfvPPA, with the left temporal lobe progressing fastest in svPPA and left frontal lobe fastest in nfvPPA (Rohrer *et al.* 2012).

Investigations of gene positive cases show a similar range of global volumetric changes but suggest that *MAPT* mutations are associated with a mean annual rate of 2.4%, intermediate between those with *GRN* mutations, who exhibit the fastest rate of loss at 3.5% and *C9orf72* whose volumetric rates are lowest at 1.4% and more in line with AD patients (Spina *et al.* 2008; Whitwell *et al.* 2011c; Mahoney *et al.* 2012a,b), although there is variability within each group. There is also some evidence for an acceleration in global rates of change in patients with non-tau pathology as disease severity increases (Whitwell *et al.* 2008); however, extensive longitudinal investigations of patients with histopathological confirmation is currently lacking.

Distinct neuroanatomical profiles from cross-sectional investigations indicate improved sensitivity may be achieved with regional analysis over global measures to capture the focal changes we might expect in FTD. However, there are currently very few studies assessing regional longitudinal rates of change and their utility in improved diagnosis and tracking of pathogenic change. A recent study applying an automated atlas-based parcellation on serial MRI demonstrated that increased annual atrophy in lateral orbitofrontal grey matter regions clearly differentiated bvFTD from both healthy controls and AD patients, whilst annual reductions in temporal lobe white matter structures were also important in classification of bvFTD subjects (Frings *et al.* 2014). More recently, cortical thickness investigation has also implicated the orbitofrontal gyrus, with significantly faster rates of regional thinning in bvFTD compared with AD and controls (Möller *et al.* 2016). Improved sensitivity for measurements of discrete white matter tract changes in the right cingulum bundle and uncinate fasciculus over more global measures has been recently reported in a longitudinal DTI investigation of bvFTD (Mahoney *et al.* 2015). Investigations in svPPA suggest improved sensitivity when measuring disease progression with temporal lobar volume change instead of hemispheric or whole-brain measurements (Rohrer *et al.* 2008a; Krueger *et al.* 2010). In addition, a recent study of progressive apraxia of speech patients (who almost exclusively present with tau pathology at post-mortem; Deramecourt *et al.* 2010; Dickson *et al.* 2010), demonstrated that annual rates of atrophy in the precentral and supplementary motor areas outperformed other regional and more global MRI measures (Whitwell *et al.* 2015).

**Table 1** Summary of annualised global and regional atrophy rates (expansion rates for ventricles) from previously published studies

Publication and cohort	Measure	bvFTD	svPPA	nvPPA	lvPPA	Controls	MAPT	GRN	C9orf72
Chan <i>et al.</i> (2001) bvFTD (n = 17), PPA (n = 13; 12 svPPA, 1 nvPPA), controls (n = 27)	Whole brain (%)	3.7 (2.5)	2.5 (1.0)			0.5 (0.4)			
Rohrer <i>et al.</i> (2008a)	Whole brain (mL)		27.4 (16.0)			4.4 (4.1)			
svPPA (n = 21), controls (n = 20)	Ventricular expansion (mL)		6.9 (3.8)			0.7 (1.0)			
	Left temporal lobe (mL)		2.8 (1.2)			0.4 (0.6)			
	Right temporal lobe (mL)		3.9 (1.7)			0.4 (0.8)			
	Left hippocampus (mL)		0.1 (0.1)			0.0 (0.1)			
	Right hippocampus (mL)		0.2 (0.1)			0.0 (0.0)			
Knopman <i>et al.</i> (2009)	Whole brain (%)	1.6 (1.1)	1.7 (1.0)	1.6 (0.9)	2.1 (1.0)	0.4 (0.4)			
bvFTD (n = 34), svPPA (n = 16), nvPPA (n = 17), lvPPA (n = 9), controls (n = 15)	Ventricular expansion (mL)	11.2 (6.8)	13.2 (5.4)	11.0 (4.4)	14.8 (5.6)	2.3 (1.4)			
Gordon <i>et al.</i> (2010)	Whole brain (%)	1.4 (1.5)	2.6 (1.6)	2.9 (0.9)		0.1 (0.5)			
bvFTD (n = 11), svPPA (n = 11), nvPPA (n = 10), controls (n = 24)	Ventricular expansion (mL)	5.5 (6.7)	7.1 (4.9)	5.6 (3.8)		0.5 (1.1)			
Rohrer <i>et al.</i> (2010b)	Whole brain (%)						1.4 (0.9–1.9)	3.4 (2.8–4.0)	
MAPT (n = 6), GRN (n = 4)									
Whitwell <i>et al.</i> (2011c)	Whole brain (%)						2.4 (1.9–2.8)	3.5 (2.8–4.2)	
MAPT (n = 12), GRN (n = 8), controls (n = 20)	Hippocampus (%)						7.8 (3.9–12.0)	6.5 (1.7–11.0)	
Rohrer <i>et al.</i> (2012)	Whole brain (%)		2.5 (1.5)	2.6 (1.2)		0.4 (0.4)			
svPPA (n = 17), nvPPA (n = 18), controls (n = 14)	Ventricular expansion (mL)		6.9 (4.4)	6.6 (3.4)		0.7 (1.2)			
	Frontal lobe (%, Left; Right)		4.3 (2.0); 2.8 (2.5)	5.7 (2.8); 4.5 (2.3)					
	Temporal lobe (%, Left; Right)		7.1 (2.3); 6.6 (2.9)	5.3 (3.6); 3.4 (3.5)					
	Parietal lobe (%, Left; Right)		3.5 (2.9); 2.0 (2.9)	4.3 (2.3); 3.5 (3.2)					
	Occipital lobe (%, Left; Right)		1.8 (3.1); 1.3 (2.9)	1.0 (3.0); 1.2 (3.8)					

(continued)

Table 1. (continued)

Publication and cohort	Measure	bvFTD	svPPA	ntvPPA	lvPPA	Controls	MAPT	GRN	C9orf72
Mahoney <i>et al.</i> (2012b) C9orf72 (n = 6), controls (n = 15)	Whole brain (%) Ventricular expansion (mL)					0.4 (0.3) 0.7 (0.6)			1.4 (1.6) 3.2 (2.0)
Frings <i>et al.</i> (2014) bvFTD (n = 15), controls (n = 10)	Lateral Orbitofrontal gyrus (%) Hippocampus & Amygdala (%) Insula (%)	5.6 (4.5) 3.6 (3.2) 3.6 (2.9) 15.2 (10.4)				1.0 (1.7) 1.0 (0.8)			
Mahoney <i>et al.</i> (2015) bvFTD (n = 23), MAPT (n = 8), C9orf72 (n = 4), controls (n = 18)	Whole brain (mL)					0.7 (0.9) 5.2 (6.7)	15.7 (6.7)		14.4 (17.8)

FA, fractional anisotropy; MD, mean diffusivity; RD, radial diffusivity; bvFTD, behavioural variant frontotemporal dementia; GRN, granulin; PPA, primary progressive aphasia; lvPPA, logopenic variant of primary progressive aphasia; MAPT, microtubule-associated protein tau; ntvPPA, non-fluent variant of primary progressive aphasia; svPPA, semantic variant of primary progressive aphasia; C9orf72, chromosome 9 open reading frame 72.

The utility of these rates of change markers, based on estimated sample sizes to demonstrate a relevant therapeutic effect, varies accordingly across method and patient subtype (Table 2). Sample sizes are generally more feasible in the PPA syndromes given the heterogeneity of bvFTD. This highlights the importance of improved stratification into trials and increasingly targeted regional measures of longitudinal change in these focal disease populations. Future confirmation of rates of change in large well-characterised cohorts is required to harmonise these longitudinal markers. However, it is promising to note that despite variability, many measures do produce feasible samples sizes of 50–100 patients per treatment arm.

### A view back in time: presymptomatic investigations

A relatively high proportion of FTD cases are familial, which provides the potential for early (presymptomatic) intervention. Presymptomatic genetic studies have suggested differential areas of earliest change across the genetic subtypes. Validating markers of these prodromal changes is essential for future trial design, because interventions in neurodegenerative conditions will ideally be prior to clinical symptoms when only minimal irreversible neuronal loss has occurred and the majority of cognitive function remains intact.

Early studies of at-risk mutation carriers reported inconsistent neuroimaging findings. Some showed evidence of grey matter atrophy in the different mutation types (Janssen *et al.* 2005; Rohrer *et al.* 2008b, 2015; Spina *et al.* 2008), whilst others found no structural MRI abnormalities prior to symptom onset (Borroni *et al.* 2008; Whitwell *et al.* 2011b; Dopper *et al.* 2013). Some of these studies did find abnormalities with the use of other imaging modalities, suggesting that changes in structural and functional connectivity may precede the development of atrophy and demonstrate greater utility as early markers. Using DTI, reduced FA in the left uncinate fasciculus and inferior fronto-occipital fasciculus was detected in four at-risk GRN patients compared with controls (Borroni *et al.* 2008). A larger DTI study also showed decreased FA in the right inferior fronto-occipital fasciculus alongside white matter abnormalities of the right anterior and superior corona radiata, anterior thalamic radiation, superior longitudinal fasciculus and internal capsule. In comparison, presymptomatic MAPT carriers demonstrated more widespread white matter abnormalities throughout frontotemporal tracts (Dopper *et al.* 2013), consistent with regions implicated in symptomatic MAPT patients. Using resting-state fMRI, this same study reported reduced functional connectivity in the anterior midcingulate cortex (part of the salience network) for GRN carriers (Dopper *et al.* 2013), whereas others have shown increased functional connectivity in the medial prefrontal cortex (Borroni *et al.* 2012), or no functional connectivity changes at all (Pievani *et al.* 2014). In MAPT mutations, reduced connectivity in the lateral temporal and prefrontal

**Table 2** Summary of previously published sample size estimates from studies investigating the use of imaging biomarkers in future clinical trials of FTD.

Publication and cohort	Measure	bvFTD	svPPA	nvPPA*	lvPPA
<b>Rohrer <i>et al.</i> (2008a)</b>					
$\beta = 90\%$ , $\alpha = 0.05$					
svPPA (n = 20, 9 FTLD-U confirmed)					
30% treatment effect	Whole brain		118		
	Ventricles		89		
	Left temporal lobe		60		
	Right temporal lobe		55		
	Left hippocampus		104		
	Right hippocampus		81		
<b>Knopman <i>et al.</i> (2009)</b>					
$\beta = 80\%$ , $\alpha = 0.05$ , correcting for					
26% attrition rate					
bvFTD (n = 34), svPPA (n = 16), nvPPA					
(n = 17), lvPPA (n = 9)					
25% treatment effect	Whole brain	165	135	105	81
	Ventricles	127	58	55	50
40% treatment effect	Whole brain	66	54	42	32
	Ventricles	51	24	23	20
<b>Gordon <i>et al.</i> (2010)</b>					
$\beta = 80\%$ , $\alpha = 0.05$ , adjusting for					
control rates and					
annual attrition of 10%					
bvFTD (n = 11), svPPA (n = 11),					
nvPPA (n = 10)					
25% treatment effect	Whole brain	360	115	26	
	Ventricles	495	157	152	
40% treatment effect	Whole brain	141	45	10	
	Ventricles	193	61	59	
<b>Rohrer <i>et al.</i> (2012)</b>					
$\beta = 90\%$ , $\alpha = 0.05$ , adjusting					
for control rates					
svPPA (n = 17), nvPPA (n = 18)					
30% treatment effect	Whole brain		120	70	
	Ventricles		118	78	
<b>Mahoney <i>et al.</i> (2015)</b>					
$\beta = 80\%$ , $\alpha = 0.05$ , adjusting					
for control rates					
bvFTD (n = 19, including 8 <i>MAPT</i> and 4					
<i>C9orf72</i> mutations)					
20% treatment effect	Whole brain	507			
	Right cingulum bundle (FA)	276			
	Right cingulum bundle (MD)	1031			
	Right uncinate fasciculus (RD)	531			
	Right uncinate fasciculus (AD)	1229			
40% treatment effect	Whole brain	127			
	Right cingulum bundle (FA)	69			
	Right cingulum bundle (MD)	258			
	Right uncinate fasciculus (RD)	133			
	Right uncinate fasciculus (AD)	308			
<b>Whitwell <i>et al.</i> (2015)</b>					
$\beta = 80\%$ , $\alpha = 0.05$					
Progressive apraxia of speech (n = 24)					

(continued)

**Table 2.** (continued)

Publication and cohort	Measure	bvFTD	svPPA	nfvPPA*	lvPPA
20% treatment effect	Precentral			38	
	Supplementary motor area			49	
	Whole brain			116	
	Ventricles			118	
	Superior frontal lobe			163	
	Superior parietal lobe			224	
	Striatum			266	
	Midbrain			380	

FA, fractional anisotropy; MD, mean diffusivity; RD, radial diffusivity; AD, axial diffusivity; bvFTD, behavioural variant frontotemporal dementia; GRN, progranulin; lvPPA, logopenic variant of primary progressive aphasia; MAPT, microtubule-associated protein tau; nfvPPA, non-fluent variant of primary progressive aphasia; svPPA, semantic variant of primary progressive aphasia; FTL-D-U, Frontotemporal lobar degeneration, with ubiquitin-positive inclusions.

The estimates represent the sample size that would be required per trial arm to detect the stated % treatment effect from measures of rates of change. The power ( $\beta$ ) and statistical threshold ( $\alpha$ ) used to calculate the sample size for each study are listed individually for every publication, as are additional factors such as controlling for normal aging and expected attrition rate from the putative trial.

\*PPAOS for Whitwell *et al.* 2015.

regions (part of the default mode network) has been reported (Whitwell *et al.* 2011b), whilst others have failed to find significant connectivity changes with these presymptomatic carriers (Dopper *et al.* 2013).

As is the nature of investigating rare forms of a rare disease, a major limitation contributing to these inconsistencies in presymptomatic research is small study sizes. To overcome this, the Genetic Frontotemporal dementia Initiative (GENFI) was launched to assess the feasibility of an international study applying uniform assessment protocols across multiple sites (Rohrer *et al.* 2015). Preliminary findings from GENFI have shown significant differences in cortical and subcortical volumes between presymptomatic carriers and non-carriers greater than 10 years before expected clinical onset. Early changes were seen in the insula, followed closely by the temporal and then frontal lobes (Fig. 7). Distinct temporal and spatial profiles were seen with the different genetic causes. For *MAPT* mutation carriers, differences first emerged in the hippocampus and amygdala (15 years before expected onset), followed by temporal lobe (10 years prior to expected onset) and insula (5 years prior). In contrast, *GRN* mutation carriers exhibited differences to non-carriers initially in the insula (15 years before onset), the temporal and parietal lobes (both 10 years before expected onset) and then striatum (5 years prior), with clear evidence of asymmetry emerging 5 years before expected symptoms. The *C9orf72* carriers presented with yet another distinct neuroanatomical profile, with subcortical regions including the thalamus, the insula and posterior cortical areas, differing from non-carriers 25 years before expected symptom onset. This was followed by the frontal and temporal lobes, both 20 years prior to onset and the cerebellum 10 years before expected symptoms.

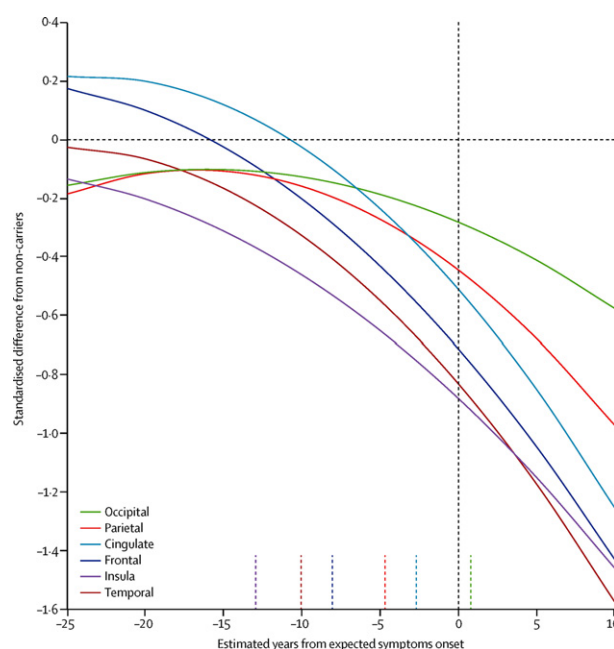


**Fig. 7** Graphs of expected trajectories of lobar change based on the standardised difference between mutation carriers and non-carriers in cortical grey matter volumetric imaging measures versus estimated years from expected symptom onset. Reproduced from Rohrer *et al.* 2015.

These regional profiles are consistent with previous neuroimaging studies in symptomatic mutation carriers, but show significant robust changes much earlier than suggested previously. As with any cross-sectional analysis, the apparent temporal and spatial sequence of disease progression is inferred from different patients in each stage of the

presymptomatic spectrum. A more robust picture of structural progression in these cortical and subcortical regions will be clarified when familial FTD studies report longitudinal data. Previous work suggests that connectivity changes precede volumetric changes and thus the inclusion of DTI and resting-state fMRI into the GENFI protocol will provide valuable information about the staging of these structural and functional changes presymptomatically. In addition, tau PET imaging shows great promise and will be invaluable for visualising and staging the evolution of pathological tau deposition throughout all stages of diseases in *MAPT* cohorts.

### A view to the future: symptomatic trial interventions

The past, present and future of FTD clinical trials is reviewed in depth elsewhere in this issue; however, a number of insights from neuroimaging in AD trials and preliminary work in FTD are worth noting. There are currently several trials targeting genetic FTD cases currently recruiting (FORUM <https://clinicaltrials.gov/ct2/show/NCT02149160>, and TauRx <https://clinicaltrials.gov/ct2/show/NCT02245568>), and the success of DIAN-TU (the Dominantly Inherited Alzheimer Network Trial) confirms the feasibility of international recruitment into presymptomatic phase II/III randomised treatment trials, incorporating multimodal imaging endpoints.

With continued development of novel and more sensitive imaging techniques, the beneficial role they can play in facilitating the design, enrolment and in assessing safety and efficacy in future clinical trials is expanding. Presymptomatic studies suggest that neuroimaging can provide valuable markers of volumetric change up to 20 years prior to expected symptom onset. The utility of structural and functional connectivity measure to contribute further to our understanding of earliest detectable changes is becoming clearer and the advent of tau PET imaging may shift the window of *in vivo* pathogenic investigation even earlier. Multimodal imaging will be an important feature of future clinical trials and its application in presymptomatic cohorts will assist in identifying the initial sites of vulnerability and in staging subsequent distribution of pathological damage in the prodromal stages of these diseases. With this in place, the optimal point of therapeutic intervention can be incorporated into future trial designs to intervene when the minimum of irreversible neuronal loss has occurred whilst still maintaining enough power to detect a positive treatment effect with inevitably relatively small study populations.

A critical trial design issue is the correct enrolment and stratification of patients who have the pathology specifically targeted by the intervention. This has been a key issue in many AD trials, which based enrolment primarily on clinical presentation without corroborating amyloid imaging. Inclusion of patients without AD pathology severely weakens the power of these studies to detect treatment effects. The same will be true for FTD trials and a combination of molecular

imaging confirmation, genotyping and probabilistic matching of the expected neuroanatomical signature of presenting patients consistent with pathology-confirmed investigations would aid in excluding patients with features indicative of other neurodegenerative conditions.

Neuroimaging markers will provide means of assessing safety by screening for adverse events. This has shown value in the detection of amyloid-relating imaging abnormalities as a response to anti-amyloid immunotherapy trials in AD (Sperling *et al.* 2011). In addition, combining available imaging will provide measures of treatment-related change in protein deposition (with tau and amyloid PET), downstream effects on functional and structural connectivity, as well as changes in regional and global measures of neuronal loss. Validation of each modality and chosen metric will be critical in the specific population targeted by the intended treatment prior to implementation. Ultimately, the absolute utility of these markers can only be confirmed in the presence of measuring a successful disease-modifying treatment. Until then, continued focus on validating these promising neuroimaging biomarkers in all stages of disease from presymptomatic through symptomatic stages of genetic and sporadic presentations to patients with histopathological confirmation will be increasingly important.

### Conclusions

The field of neuroimaging in FTD has made significant advances over the past 5 years. These have been driven by improved understanding of the underlying genetics and pathology, alongside improvements in imaging and in particular the development of molecular imaging of tau. With a renewed focus on longitudinal investigations, the use of combined imaging modalities on large well-characterised cohorts, and the development of therapeutic trials that incorporate multi-modal imaging, the next 5 years hold promise for even greater insights from imaging in FTD.

### Acknowledgments and conflict of interest disclosure

This work was funded by Medical Research Council (Grant/Award Number: MR/M008525/1). The authors have no conflict of interest to declare.

### References

- Agosta F., Canu E., Sarro L., Comi G. and Filippi M. (2012a) Neuroimaging findings in frontotemporal lobar degeneration spectrum of disorders. *Cortex* **48**, 389–413.
- Agosta F., Scola E., Canu E., *et al.* (2012b) White matter damage in frontotemporal lobar degeneration spectrum. *Cereb. Cortex* **22**, 2705–2714.
- Agosta F., Galantucci S., Valsasina P., Canu E., Meani A., Marcone A., Magnani G., Falini A., Comi G. and Filippi M. (2014) Disrupted

- brain connectome in semantic variant of primary progressive aphasia. *Neurobiol. Aging* **35**, 2646–2655.
- Avants B. B., Cook P. A., Ungar L., Gee J. C. and Grossman M. (2010) Dementia induces correlated reductions in white matter integrity and cortical thickness: A multivariate neuroimaging study with sparse canonical correlation analysis. *NeuroImage* **50**, 1004–1016.
- Binnewijzend M. A. A., Kuijter J. P. A., van der Flier W. M., et al. (2014) Distinct perfusion patterns in Alzheimer's disease, frontotemporal dementia and dementia with Lewy bodies. *Eur. Radiol.* **24**, 2326–2333.
- Bohnen N. I., Djang D. S. W., Herholz K., Anzai Y. and Minoshima S. (2012) Effectiveness and safety of 18F-FDG PET in the evaluation of dementia: a review of the recent literature. *J. Nucl. Med.* **53**, 59–71.
- Borroni B., Alberici A., Premi E., Archetti S., Garibotto V., Agosti C., Gasparotti R., Luca M., Di Perani D. and Padovani A. (2008) Brain magnetic resonance imaging structural changes in a pedigree of asymptomatic progranulin mutation carriers. *Rejuvenation Res.* **11**, 585–595.
- Borroni B., Alberici A., Cercignani M., et al. (2012) Granulin mutation drives brain damage and reorganization from preclinical to symptomatic FTL D. *Neurobiol. Aging* **33**, 2506–2520.
- Brambati S. M., Rankin K. P., Narvid J., Seeley W. W., Dean D. L., Rosen H. J., Miller B. L., Ashburner J. and Gorno-Tempini M. L. (2009) Atrophy progression in semantic dementia with asymmetric temporal involvement: A tensor-based morphometry study. *Neurobiol. Aging* **30**, 103–111.
- Cash D. M., Rohrer J. D., Ryan N. S., Ourselin S. and Fox N. C. (2014) Imaging endpoints for clinical trials in Alzheimer's disease. *Alzheimers. Res. Ther.* **6**, 87–97.
- Catani M. and Mesulam M. (2008) The arcuate fasciculus and the disconnection theme in language and aphasia: history and current state. *Cortex* **44**, 953–961.
- Cerami C. and Cappa S. F. (2013) The behavioral variant of frontotemporal dementia: linking neuropathology to social cognition. *Neurol. Sci.* **34**, 1267–1274.
- Chan D., Fox N. C., Jenkins R., Schill R. I., Crum W. R. and Rossor M. N. (2001) Rates of global and regional cerebral atrophy in AD and frontotemporal dementia. *Neurology* **57**, 1756–1763.
- Chan D., Anderson V., Pijnenburg Y., et al. (2009) The clinical profile of right temporal lobe atrophy. *Brain* **132**, 1287–1298.
- Chien D. T., Bahri S., Szardenings A. K., Walsh J. C., Mu F., Su M.-Y., Shankle W. R., Elizarov A. and Kolb H. C. (2013) Early clinical PET imaging results with the novel PHF-tau radioligand [F-18]-T807. *J. Alzheimers Dis.* **34**, 457–468.
- Chien D. T., Szardenings A. K., Bahri S., et al. (2014) Early clinical PET imaging results with the novel PHF-tau radioligand [F18]-T808. *J. Alzheimer's Dis.* **38**, 171–184.
- Davison C. M. and O'Brien J. T. (2014) A comparison of FDG-PET and blood flow SPECT in the diagnosis of neurodegenerative dementias: A systematic review. *Int. J. Geriatr. Psychiatry* **29**, 551–561.
- Deramecourt V., Lebert F., Buee L., Maurage C. A. and Pasquier F. (2010) Prediction of pathology in primary progressive language and speech disorders. *Alzheimer's Dement.* **74**, 42–49.
- Desgranges B., Matuszewski V., Piolino P., Chételat G., Mézenge F., Landeau B., La Sayette V., De Belliard S. and Eustache F. (2007) Anatomical and functional alterations in semantic dementia: a voxel-based MRI and PET study. *Neurobiol. Aging* **28**, 1904–1913.
- Dickson D. W., Ahmed Z., Algom A. A., Tsuboi Y. and Josephs K. A. (2010) Neuropathology of variants of progressive supranuclear palsy. *Curr. Opin. Neurol.* **23**, 394–400.
- Diehl-Schmid J., Grimmer T., Drzezga A., Bornschein S., Perneczky R., Förstl H., Schwaiger M. and Kurz A. (2006) Longitudinal changes of cerebral glucose metabolism in semantic dementia. *Dement. Geriatr. Cogn. Disord.* **22**, 346–351.
- Diehl-Schmid J., Grimmer T., Drzezga A., Bornschein S., Riemenschneider M., Förstl H., Schwaiger M. and Kurz A. (2007) Decline of cerebral glucose metabolism in frontotemporal dementia: a longitudinal 18F-FDG-PET-study. *Neurobiol. Aging* **28**, 42–50.
- Diehl-Schmid J., Onur O. A., Kuhn J., Gruppe T. and Drzezga A. (2014) Imaging frontotemporal lobar degeneration. *Curr Neurol Neurosci Rep.* 2014 Oct; **14**(10): 489–499.
- Dopper E. G. P., Rombouts S. A. R. B., Jiskoot L. C., et al. (2013) Structural and functional brain connectivity in presymptomatic familial frontotemporal dementia. *Neurology* **80**, 814–823.
- Drzezga A., Grimmer T., Henriksen G., Stangier I., Perneczky R., Diehl-Schmid J., Mathis C. A., Klunk W. E., Price J. and DeKosky S. (2008) Imaging of amyloid plaques and cerebral glucose metabolism in semantic dementia and Alzheimer's disease. *NeuroImage* **39**, 619–633.
- Engler H., Santillo A. F., Wang S. X., Lindau M., Savitcheva I., Nordberg A., Lannfelt L., Långström B. and Kilander L. (2008) In vivo amyloid imaging with PET in frontotemporal dementia. *Eur. J. Nucl. Med. Mol. Imaging* **35**, 100–106.
- Farb N. A. S., Grady C. L., Strother S., et al. (2013) Abnormal network connectivity in frontotemporal dementia: evidence for prefrontal isolation. *Cortex* **49**, 1856–1873.
- Filippi M., Agosta F., Scola E., et al. (2013) Functional network connectivity in the behavioral variant of frontotemporal dementia. *Cortex* **49**, 2389–2401.
- Foster N. L., Heidebrink J. L., Clark C. M., et al. (2007) FDG-PET improves accuracy in distinguishing frontotemporal dementia and Alzheimer's disease. *Brain* **130**, 2616–2635.
- Freeborough P. A. and Fox N. C. (1997) The boundary shift integral: an accurate and robust measure of cerebral volume changes from registered repeat MRI. *IEEE Trans. Med. Imaging* **16**, 623–629.
- Frings L., Yew B., Flanagan E., Lam B. Y. K., Hüll M., Huppertz H.-J., Hodges J. R. and Hornberger M. (2014) Longitudinal grey and white matter changes in frontotemporal dementia and Alzheimer's disease. *PLoS ONE* **9**, e90814.
- Galantucci S., Tartaglia M. C., Wilson S. M., et al. (2011) White matter damage in primary progressive aphasia: a diffusion tensor tractography study. *Brain* **134**, 3011–3029.
- Ghetti B., Oblak A. L., Boeve B. F., Johnson K. A., Dickerson B. C. and Goedert M. (2015) Invited review: Frontotemporal dementia caused by microtubule-associated protein tau gene (MAPT) mutations: a chameleon for neuropathology and neuroimaging. *Neuropathol. Appl. Neurobiol.* **41**, 24–46.
- Gordon E., Rohrer J. D., Kim L. G., Omar R., Rossor M. N., Fox N. C. and Warren J. D. (2010) Measuring disease progression in frontotemporal lobar degeneration: A clinical and MRI study. *Neurology* **74**, 666–673.
- Gorno-Tempini M. L., Dronkers N. F., Rankin K. P., Ogar J. M., Phengrasamy L., Rosen H. J., Johnson J. K., Weiner M. W. and Miller B. L. (2004) Cognition and anatomy in three variants of primary progressive aphasia. *Ann. Neurol.* **55**, 335–346.
- Gorno-Tempini M. L., Hillis A. E., Weintraub S., et al. (2011) Classification of primary progressive aphasia and its variants. *Neurology* **76**, 1006–1014.
- Guo C. C., Gorno-Tempini M. L., Gesierich B., et al. (2013) Anterior temporal lobe degeneration produces widespread network-driven dysfunction. *Brain* **136**, 2979–2991.
- Hoefl F., Gabrieli J. D. E., Whitfield-Babrieli S., Haas B. W., Bammer R., Menon V. and Spiegel D. (2012) Functional brain basis of Hypnotizability. *Arch. Gen. Psychiatry* **69**, 1064–1072.

- Hu W. T., Wang Z., Lee V. M.-Y., Trojanowski J. Q., Detre J. A. and Grossman M. (2010) Distinct cerebral perfusion patterns in FTLTD and AD. *Neurology* **75**, 881–888.
- Ishii K. (2014) PET approaches for diagnosis of dementia. *AJNR Am. J. Neuroradiol.* **35**, 2030–2038.
- Jack C. R., Knopman D. S., Jagust W. J., Shaw L. M., Aisen P. S., Weiner M. W., Petersen R. C. and Trojanowski J. Q. (2010) Hypothetical model of dynamic biomarkers of the Alzheimer's pathological cascade. *Lancet Neurol.* **9**, 119–128.
- Janssen J. C., Schott J. M., Cipelotti L., Fox N. C., Scahill R. I., Josephs K. A., Stevens J. M. and Rossor M. N. (2005) Mapping the onset and progression of atrophy in familial frontotemporal lobar degeneration. *J. Neurol. Neurosurg. Psychiatry* **76**, 162–168.
- Josephs K. A., Whitwell J. L., Dickson D. W., Boeve B. F., Knopman D. S., Petersen R. C., Parisi J. E. and Jack C. R. (2008) Voxel-based morphometry in autopsy proven PSP and CBD. *Neurobiol. Aging* **29**, 280–289.
- Josephs K. A., Whitwell J. L., Knopman D. S., *et al.* (2009) Two distinct subtypes of right temporal variant frontotemporal dementia. *Neurology* **73**, 1443–1450.
- Josephs K. A., Whitwell J. L., Parisi J. E., Petersen R. C., Boeve B. F., Jack C. R. and Dickson D. W. (2010) Caudate atrophy on MRI is a characteristic feature of FTLTD-FUS. *Eur. J. Neurol.* **17**, 969–975.
- Josephs K. A., Duffy J. R., Strand E. A., *et al.* (2014) Progranulin-associated PiB-negative logopenic primary progressive aphasia. *J. Neurol.* **261**, 604–614.
- Kim E.-J., Park Y.-E., Kim D.-S., *et al.* (2011) Inclusion body myopathy with Paget disease of bone and frontotemporal dementia linked to VCP p.Arg155Cys in a Korean family. *Arch. Neurol.* **68**, 787–796.
- Knopman D. S., Jack C. R., Kramer J. H., Boeve B. F., Caselli R. J., Graff-Radford N. R., Mendez M. F., Miller B. L. and Mercaldo N. D. (2009) Brain and ventricular volumetric changes in frontotemporal lobar degeneration over 1 year. *Neurology* **72**, 1843–1849.
- Krueger C. E., Dean D. L., Rosen H. J., Halabi C., Weiner M. W., Miller B. L. and Kramer J. H. (2010) Longitudinal rates of lobar atrophy in frontotemporal dementia, semantic dementia, and Alzheimer's disease. *Alzheimer Dis. Assoc. Disord.* **24**, 43–48.
- Lam B. Y. K., Halliday G. M., Irish M., Hodges J. R. and Piguet O. (2014) Longitudinal white matter changes in frontotemporal dementia subtypes. *Hum. Brain Mapp.* **35**, 3547–3557.
- Lee S. E., Khazenzon A. M., Trujillo A. J., *et al.* (2014) Altered network connectivity in frontotemporal dementia with C9orf72 hexanucleotide repeat expansion. *Brain* **137**, 3047–3060.
- Leyton C. E., Villemagne V. L., Savage S., Pike K. E., Ballard K. J., Piguet O., Burrell J. R., Rowe C. C. and Hodges J. R. (2011) Subtypes of progressive aphasia: application of the international consensus criteria and validation using  $\beta$ -amyloid imaging. *Brain* **134**, 3030–3043.
- Liang Y., Gordon E., Rohrer J., *et al.* (2014) A cognitive chameleon: lessons from a novel MAPT mutation case. *Neurocase* **20**, 684–694.
- Mackenzie I. R. A., Neumann M., Bigio E. H., *et al.* (2010) Nomenclature and nosology for neuropathologic subtypes of frontotemporal lobar degeneration: an update. *Acta Neuropathol.* **119**, 1–4.
- Mackenzie I. R. A., Neumann M., Baborie A., Sampathu D. M., Plessis D., Du Jaros. E., Perry R. H., Trojanowski J. Q., Mann D. M. A. and Lee V. M. Y. (2011) A harmonized classification system for FTLTD-TDP pathology. *Acta Neuropathol.* **122**, 111–113.
- Madhavan A., Whitwell J. L., Weigand S. D., *et al.* (2013) FDG PET and MRI in Logopenic Primary Progressive Aphasia versus Dementia of the Alzheimer's Type. *PLoS ONE* **8**, e62471.
- Mahoney C. J., Beck J., Rohrer J. D., *et al.* (2012a) Frontotemporal dementia with the C9ORF72 hexanucleotide repeat expansion: clinical, neuroanatomical and neuropathological features. *Brain* **135**, 736–750.
- Mahoney C. J., Downey L. E., Ridgway G. R., *et al.* (2012b) Longitudinal neuroimaging and neuropsychological profiles of frontotemporal dementia with C9ORF72 expansions. *Alzheimers. Res. Ther.* **4**, 41–51.
- Mahoney C. J., Malone I. B., Ridgway G. R., *et al.* (2013) White matter tract signatures of the progressive aphasias. *Neurobiol. Aging* **34**, 1687–1699.
- Mahoney C. J., Ridgway G. R., Malone I. B., *et al.* (2014) Profiles of white matter tract pathology in frontotemporal dementia. *Hum. Brain Mapp.* **35**, 4163–4179.
- Mahoney C. J., Simpson I. J. A., Nicholas J. M., *et al.* (2015) Longitudinal diffusion tensor imaging in frontotemporal dementia. *Ann. Neurol.* **77**, 33–46.
- Massey L. A., Jager H. R., Paviour D. C., *et al.* (2013) The midbrain to pons ratio: A simple and specific MRI sign of progressive supranuclear palsy. *Neurology* **80**, 1856–1861.
- Matias-Guiu J. A., Cabrera-Martín M. N., García-Ramos R., Moreno-Ramos T., Valles-Salgado M., Carreras J. L. and Matias-Guiu J. (2014) Evaluation of the new consensus criteria for the diagnosis of primary progressive aphasia using fluorodeoxyglucose positron emission tomography. *Dement. Geriatr. Cogn. Disord.* **38**, 147–152.
- McMillan C. T., Brun C., Siddiqui S., Churgin M., Libon D., Yushkevich P., Zhang H., Boller A., Gee J. and Grossman M. (2012) White matter imaging contributes to the multimodal diagnosis of frontotemporal lobar degeneration. *Neurology* **78**, 1761–1768.
- McMillan C. T., Avants B., Irwin D. J., Toledo J. B., Wolk D. A., Van Deerlin V. M., Shaw L. M., Trojanowski J. Q. and Grossman M. (2013a) Can MRI screen for CSF biomarkers in neurodegenerative disease? *Neurology* **80**, 132–138.
- McMillan C. T., Irwin D. J., Avants B. B., *et al.* (2013b) White matter imaging helps dissociate tau from TDP-43 in frontotemporal lobar degeneration. *J. Neurol. Neurosurg. Psychiatry* **84**, 949–955.
- McMillan C. T., Avants B. B., Cook P., Ungar L., Trojanowski J. Q. and Grossman M. (2014) The power of neuroimaging biomarkers for screening frontotemporal dementia. *Hum. Brain Mapp.* **35**, 4827–4840.
- Mesulam M. M., Weintraub S., Rogalski E. J., Wieneke C., Geula C. and Bigio E. H. (2014) Asymmetry and heterogeneity of Alzheimer's and frontotemporal pathology in primary progressive aphasia. *Brain* **137**, 1176–1192.
- Möller C., Hafkemeijer A., Pijnenburg Y. A. L., *et al.* (2016) Different patterns of cortical gray matter loss over time in behavioral variant frontotemporal dementia and Alzheimer's disease. *Neurobiol. Aging* **38**, 21–31.
- Mosconi L., Tsui W. H., Herholz K., *et al.* (2008) Multicenter standardized 18 F-FDG PET diagnosis of mild cognitive impairment, Alzheimer's disease, and other dementias. *J. Nucl. Med.* **49**, 390–398.
- Onyike C. U. and Diehl-Schmid J. (2013) The epidemiology of frontotemporal dementia. *Int. Rev. Psychiatry* **25**, 130–137.
- Pan P. L., Song W., Yang J., Huang R., Chen K., Gong Q. Y., Zhong J. G., Shi H. C. and Sang H. F. (2012) Gray matter atrophy in behavioral variant frontotemporal dementia: a meta-analysis of voxel-based morphometry studies. *Dement. Geriatr. Cogn. Disord.* **33**, 141–148.
- Panegyres P. K., Rogers J. M., McCarthy M., Campbell A. and Wu J. S. (2009) Fluorodeoxyglucose-positron emission tomography in the differential diagnosis of early-onset dementia: a prospective, community-based study. *BMC Neurol.* 2009 Aug 12; **9**: 41–50.

- Pievani M., Paternicò D., Benussi L., Binetti G., Orlandini A., Cobelli M., Magnaldi S., Ghidoni R. and Frisoni G. B. (2014) Pattern of structural and functional brain abnormalities in asymptomatic granulin mutation carriers. *Alzheimer's Dement.* **10**, 354–364.
- Rabinovici G. D., Jagust W. J., Furst A. J., et al. (2008) Abeta amyloid and glucose metabolism in three variants of primary progressive aphasia. *Ann. Neurol.* **64**, 388–401.
- Rabinovici G. D., Rosen H. J., Alkalay A., et al. (2011) Amyloid vs FDG-PET in the differential diagnosis of AD and FTL. *Neurology* **77**, 2034–2042.
- Rankin K. P., Mayo M. C., Seeley W. W., et al. (2011) Behavioral variant frontotemporal dementia with corticobasal degeneration pathology: phenotypic comparison to bvFTD with Pick's disease. *J. Mol. Neurosci.* **45**, 594–608.
- Rogalski E. J., Cobia D., Harrison T. M., Wieneke C., Weintraub S. and Mesulam M. M. (2011) Progression of language decline and cortical atrophy in subtypes of primary progressive aphasia. *Neurology* **76**, 1804–1810.
- Rohrer J. D. and Rosen H. J. (2013) Neuroimaging in frontotemporal dementia. *Int. Rev. Psychiatry* **25**, 221–229.
- Rohrer J. D., McNaught E., Foster J., Clegg S., Barnes J., Omar R., Warrington E., Rossor M. N., Warren J. D. and Fox N. C. (2008a) Tracking progression in frontotemporal lobar degeneration: serial MRI in semantic dementia. *Neurology* **71**, 1445–1451.
- Rohrer J. D., Warren J. D., Barnes J., et al. (2008b) Mapping the progression of progranulin-associated frontotemporal lobar degeneration. *Nat. Clin. Pract. Neurol.* **4**, 455–460.
- Rohrer J. D., Guerreiro R., Vandrovicova J., et al. (2009a) The heritability and genetics of frontotemporal lobar degeneration. *Neurology* **73**, 1451–1456.
- Rohrer J. D., Warren J. D., Modat M., Ridgway G. R., Douiri A., Rossor M. N., Ourselin S. and Fox N. C. (2009b) Patterns of cortical thinning in the language variants of frontotemporal lobar degeneration. *Neurology* **72**, 1562–1569.
- Rohrer J. D., Geser F., Zhou J., Gennatas E. D., Sidhu M., Trojanowski J. Q., Dearmond S. J., Miller B. L. and Seeley W. W. (2010a) TDP-43 subtypes are associated with distinct atrophy patterns in frontotemporal dementia. *Neurology* **75**, 2204–2211.
- Rohrer J. D., Ridgway G. R., Modat M., Ourselin S., Mead S., Fox N. C., Rossor M. N. and Warren J. D. (2010b) Distinct profiles of brain atrophy in frontotemporal lobar degeneration caused by progranulin and tau mutations. *NeuroImage* **53**, 1070–1076.
- Rohrer J. D., Lashley T., Schott J. M., et al. (2011) Clinical and neuroanatomical signatures of tissue pathology in frontotemporal lobar degeneration. *Brain* **134**, 2565–2581.
- Rohrer J. D., Clarkson M. J., Kittus R., Rossor M. N., Ourselin S., Warren J. D. and Fox N. C. (2012) Rates of hemispheric and lobar atrophy in the language variants of frontotemporal lobar degeneration. *J. Alzheimers Dis.* **30**, 407–411.
- Rohrer J. D., Nicholas J. M., Cash D. M., et al. (2015) Presymptomatic cognitive and neuroanatomical changes in genetic frontotemporal dementia in the Genetic Frontotemporal dementia Initiative (GENFI) study: a cross-sectional analysis. *Lancet Neurol.* **14**, 253–262.
- Schroeter M. L., Raczka K., Neumann J. and Yves von Cramon D. (2007) Towards a nosology for frontotemporal lobar degenerations-A meta-analysis involving 267 subjects. *NeuroImage* **36**, 497–510.
- Schroeter M. L., Laird A. R., Chwiesko C., Deuschl C., Schneider E., Bzdok D., Eickhoff S. B. and Neumann J. (2014) Conceptualizing neuropsychiatric diseases with multimodal data-driven meta-analyses - The case of behavioral variant frontotemporal dementia. *Cortex* **57**, 22–37.
- Seelaar H., Klijnsma K. Y., deKoning I., dervan Lugt A., Chiu W. Z., Azmani A., Rozemuller A. J. M. and vanSwieten J. C. (2010) Frequency of ubiquitin and FUS-positive, TDP-43-negative frontotemporal lobar degeneration. *J. Neurol.* **257**, 747–753.
- Seelaar H., Rohrer J. D., Pijnenburg Y. A. L., Fox N. C. and vanSwieten J. C. (2011) Clinical, genetic and pathological heterogeneity of frontotemporal dementia: a review. *J. Neurol. Neurosurg. Psychiatry* **82**, 476–486.
- Seeley W. W., Menon V., Schatzberg A. F., Keller J., Glover G. H., Kenna H., Reiss A. L. and Greicius M. D. (2007) Dissociable intrinsic connectivity networks for salience processing and executive control. *J. Neurosci.* **27**, 2349–2356.
- Seeley W. W., Crawford R. K., Zhou J., Miller B. L. and Greicius M. D. (2009) Neurodegenerative diseases target large-scale human brain networks. *Neuron* **62**, 42–52.
- Sergeant N., Bretteville A., Hamdane M., et al. (2008) Biochemistry of Tau in Alzheimer's disease and related neurological disorders. *Expert Rev. Proteomics* **5**, 207–224.
- Serrano G. E., Sabbagh M. N., Sue L. I., et al. (2014) Positive florbetapir PET amyloid imaging in a subject with frequent cortical neuritic plaques and frontotemporal lobar degeneration with TDP43-positive inclusions. *J. Alzheimers Dis.* **42**, 813–821.
- Sha S. J., Takada L. T., Rankin K. P., et al. (2012) Frontotemporal dementia due to C9ORF72 mutations: Clinical and imaging features. *Neurology* **79**, 1002–1011.
- Shimizu S., Zhang Y., Laxamana J., Miller B. L., Kramer J. H., Weiner M. W. and Schuff N. (2010) Concordance and discordance between brain perfusion and atrophy in frontotemporal dementia. *Brain Imaging Behav.* **4**, 46–54.
- Soares J. M., Marques P., Alves V. and Sousa N. (2013) A hitchhiker's guide to diffusion tensor imaging. *Front. Neurosci.* **7**, 1–14.
- Sperling R., Jack C. R., Black S. E., et al. (2011) Amyloid related imaging abnormalities in amyloid modifying therapeutic trials: Recommendations from the Alzheimer's Association Research Roundtable Workgroup. *Alzheimer's Dement.* **7**, 367–385.
- Spina S., Farlow M. R., Unverzagt F. W., et al. (2008) The tauopathy associated with mutation +3 in intron 10 of Tau: characterization of the MSTD family. *Brain* **131**, 72–89.
- Steketee R. M. E., Bron E. E., Meijboom R., et al. (2015) Early-stage differentiation between presenile Alzheimer's disease and frontotemporal dementia using arterial spin labeling MRI. *Eur. Radiol.* **26**, 244–253.
- Stojkovic T., Hammouda E. H., Richard P., et al. (2009) Clinical outcome in 19 French and Spanish patients with valosin-containing protein myopathy associated with Paget's disease of bone and frontotemporal dementia. *Neuromuscul. Disord.* **19**, 316–323.
- Surampalli A., Gold B. T., Smith C., et al. (2015) A case report comparing clinical, imaging and neuropsychological assessment findings in twins discordant for the VCP p. R155C mutation. *Neuromuscul. Disord.* **25**, 177–183.
- Tolboom N., Koedam E. L. G. E., Schott J. M., Yaqub M., Blankenstein M. A., Barkhof F., Pijnenburg Y. A. L., Lammertsma A. A., Scheltens P. and van Berckel B. N. M. (2010) Dementia mimicking Alzheimer's disease Owing to a tau mutation: CSF and PET findings. *Alzheimer Dis. Assoc. Disord.* **24**, 303–307.
- Tu S., Leyton C. E., Hodges J. R., Piguet O. and Hornberger M. (2016) Divergent longitudinal propagation of white matter degradation in logopenic and semantic variants of primary progressive aphasia. *J. Alzheimers Dis.* **49**, 853–861.
- Verfaillie S. C. J., Adriaanse S. M., Binnewijzend M. A. A., et al. (2015) Cerebral perfusion and glucose metabolism in Alzheimer's disease and frontotemporal dementia: two sides of the same coin? *Eur. Radiol.* **25**, 3050–3059.
- Villemagne V. L. and Okamura N. (2014) In vivo tau imaging: Obstacles and progress. *Alzheimer's Dement.* **10**, S254–S264.

- Villemagne V. L. and Okamura N. (2016) Tau imaging in the study of ageing, Alzheimer's disease, and other neurodegenerative conditions. *Curr. Opin. Neurobiol.* **36**, 43–51.
- Villemagne V. L., Ong K., Mulligan R. S., *et al.* (2011) Amyloid imaging with 18F-florbetaben in Alzheimer disease and other dementias. *J. Nucl. Med.* **52**, 1210–1217.
- Villemagne V. L., Furumoto S., Fodero-Tavoletti M. T., *et al.* (2014) In vivo evaluation of a novel tau imaging tracer for Alzheimer's disease. *Eur. J. Nucl. Med. Mol. Imaging* **41**, 816–826.
- Villemagne V. L., Fodero-Tavoletti M. T., Masters C. L. and Rowe C. C. (2015) Tau imaging: early progress and future directions. *Lancet Neurol.* **14**, 114–124.
- Warren J. D., Rohrer J. D., Schott J. M., Fox N. C., Hardy J. and Rossor M. N. (2013) Molecular nexopathies: A new paradigm of neurodegenerative disease. *Trends Neurosci.* **36**, 561–569.
- Whitwell J. L., Jack C. R., Pankratz V. S., Parisi J. E., Knopman D. S., Boeve B. F., Petersen R. C., Dickson D. W. and Josephs K. A. (2008) Rates of brain atrophy over time in autopsy-proven frontotemporal dementia and Alzheimer disease. *NeuroImage* **39**, 1034–1040.
- Whitwell J. L., Jack C. R., Boeve B. F., *et al.* (2009a) Atrophy patterns in IVS10+16, IVS10+3, N279K, S305N, P301L, and V337M MAPT mutations. *Neurology* **73**, 1058–1065.
- Whitwell J. L., Przybelski S. A. and Weigand S. D., *et al.* (2009b) Distinct anatomical subtypes of the behavioural variant of frontotemporal dementia: a cluster analysis study. *Brain* **132**, 2932–2946.
- Whitwell J. L., Jack C. R., Boeve B. F., *et al.* (2010a) Imaging correlates of pathology in corticobasal syndrome. *Neurology* **75**, 1879–1887.
- Whitwell J. L., Jack C. R., Parisi J. E., *et al.* (2010b) Does TDP-43 type confer a distinct pattern of atrophy in frontotemporal lobar degeneration? *Neurology* **75**, 2212–2220.
- Whitwell J. L., Jack C. R., Parisi J. E., Knopman D. S., Boeve B. F., Petersen R. C., Dickson D. W. and Josephs K. A. (2011a) Imaging signatures of molecular pathology in behavioral variant frontotemporal dementia. *J. Mol. Neurosci.* **45**, 372–378.
- Whitwell J. L., Josephs K. A., Avula R., *et al.* (2011b) Altered functional connectivity in asymptomatic MAPT subjects. *A comparison to bvFTD. Neurology* **77**, 866–874.
- Whitwell J. L., Weigand S. D., Gunter J. L., *et al.* (2011c) Trajectories of brain and hippocampal atrophy in FTD with mutations in MAPT or GRN. *Neurology* **77**, 393–398.
- Whitwell J. L., Weigand S. D., Boeve B. F., *et al.* (2012) Neuroimaging signatures of frontotemporal dementia genetics: C9ORF72, tau, progranulin and sporadics. *Brain* **135**, 794–806.
- Whitwell J. L., Duffy J. R., Strand E. A., *et al.* (2015) Sample size calculations for clinical trials targeting tauopathies: a new potential disease target. *J. Neurol.* **262**, 2064–2072.
- Xia C.-F., Arteaga J., Chen G., *et al.* (2013) [18F]JIT807, a novel tau positron emission tomography imaging agent for Alzheimer's disease. *Alzheimer's Dement.* **9**, 666–676.
- Zhang Y., Schuff N., Ching C., *et al.* (2011) Joint assessment of structural, perfusion, and diffusion MRI in Alzheimer's disease and frontotemporal dementia. *Int. J. Alzheimers. Dis.* **2011**, doi:10.4061/2011/546871.
- Zhou J. and Seeley W. W. (2014) Network dysfunction in Alzheimer's disease and frontotemporal dementia: Implications for psychiatry. *Biol. Psychiatry* **75**, 565–573.
- Zhou J., Greicius M. D., Gennatas E. D., Growdon M. E., Jang J. Y., Rabinovici G. D., Kramer J. H., Weiner M., Miller B. L. and Seeley W. W. (2010) Divergent network connectivity changes in behavioural variant frontotemporal dementia and Alzheimer's disease. *Brain* **133**, 1352–1367.